

# Transport parameter estimation in homogeneous and two-layered porous media using two different methods: genetic algorithm and image analysis

K. Inoue<sup>1</sup>, I. Masaki<sup>2</sup>, Y. Shimada<sup>1</sup> & T. Tanaka<sup>1</sup>

<sup>1</sup>*Faculty of Agriculture, Kobe University, Japan*

<sup>2</sup>*Graduate School of Science and Technology, Kobe University, Japan*

## Abstract

Laboratory tracer experiments are conducted in homogeneous and two-layered flow fields under various hydraulic gradient conditions. NaCl solution dyed with Brilliant Blue FCF is used as a tracer in order to measure NaCl breakthrough curves and obtain images of dye tracer movement. Inverse analysis through genetic algorithm and image analysis are employed to estimate dispersivity, dispersion coefficient and retardation factor. The results show that dispersivity estimated from image analysis is about one order smaller than that of GA estimates. Moreover, it is revealed that tracer is slightly retarded relative to pore water velocity. As for parameter estimation in two-layered media, the values of equivalent dispersivity to the entire flow region exist between the values estimated in each layer. Estimated dispersivity in layered media depends on transport pathway of contaminant, suggesting the importance of observation location in parameter estimation problem.

*Keywords: tracer experiment, parameter estimation, inverse analysis, genetic algorithm, image analysis, dispersivity, retardation factor.*

## 1 Introduction

Several contaminants have been found in groundwater and the behavior of contaminants in the subsurface involves several different and simultaneous phenomena. Advection and dispersion, which are of significance in solute transport phenomena, play an important role in assessment or prediction of groundwater



contamination. Additionally, adsorption of contaminants to a soil particle is also key to understand the fate of contaminant.

Various experimental studies have been conducted to estimate dispersivity in column or flow-tank experiments (Huang *et al.* [1]; Robbins [2]). In such experiments, NaCl or KBr solution have frequently used as a tracer to measure its breakthrough curves. Then, dispersivity has been estimated based on breakthrough curves using inverse analysis linked with the advection-dispersion equation. However, as for an acquisition of concentration data, a relatively large sampling volume or installed measuring devices may be required and disturb flow paths. Also, tracer concentrations are often diluted in the process of gaining concentration data. To overcome these difficulties, dye tracers have been used to stain flow pathway and visually understand tracer movement (Forrer *et al.* [3]). In this study, laboratory tracer experiments are carried out in horizontally packed homogeneous flow field with the tracer of NaCl solution dyed with Brilliant Blue FCF. One objective of the present study is to estimate transport parameters using inverse analysis through genetic algorithm (GA) linked with an analytical solution of the advection-dispersion equation and image analysis based on a time series of digitized images.

As for dispersivity, it is traditionally considered possible to describe layered porous formation by means of spatial averages of the local properties over the domain. Although estimation of transport parameters is based on the assumption that concerning fields are homogeneous, inherently field soils are in heterogeneous in space. In this study, the case of two-layered porous media is of interest as a stepping stone to heterogeneous porous media. Second objective of this study is to investigate equivalent dispersivity in two-layered flow field compared to that in homogeneous flow field.

## 2 Tracer experiments

### 2.1 Materials and experimental apparatus

Tracer experiments are performed in a horizontally placed water tank with 100 cm long and 50 cm wide. The tank contains a soil sample of 6 cm thick and consists of four stainless steel sidewalls with mesh at the bottom, and a 1.0 cm thick acrylic plate at the top. The plan view of experimental apparatus is shown in Figure 1. Constant head water reservoirs connected to the upstream and downstream ends of the tank are used to control hydraulic gradient. In order to measure the piezometric head, 20 piezometric water pressure measurement ports are installed at the bottom of the tank. While transparent acrylic plate allows visualizing the profile of migration of dye tracer with a digital camera, NaCl sensors are inserted to observe its concentration.

NaCl solution of 5 mg/cm<sup>3</sup> concentration dyed with Brilliant Blue FCF of 5 mg/cm<sup>3</sup> concentration is used as a tracer to obtain NaCl breakthrough curves, to apply the parameter estimation and to characterize the movement of Brilliant Blue FCF. Although the initial concentration of tracer is determined to be low enough to



Table 1: Properties of sands used in the experiment.

Material	Particle density (g/cm <sup>3</sup> )	Hydraulic conductivity (cm/s)	Porosity (-)	Mean particle size (cm)	Uniformity coefficient (-)
Sand A	2.68	$7.51 \times 10^{-1}$	0.41	$8.5 \times 10^{-2}$	1.80
Sand B	2.66	$2.68 \times 10^{-1}$	0.41	$5.0 \times 10^{-2}$	1.25

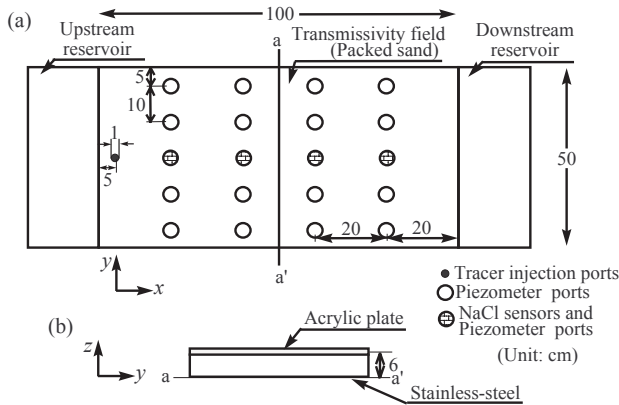


Figure 1: Schematic diagram of the experimental apparatus. (a) Plan view. (b) a-a' cross section.

avoid density-induced flow effects, there is no completely denying that the effect of gravity on solute transport in a horizontal flow.

To investigate the influence of particle size of sand on solute transport phenomena, two types of silica sand materials are used. According to the difference of the average particle size, these sands are named Sand A and B. Properties of sand materials such as particle density, the hydraulic conductivity at saturation, porosity, mean particle size, and uniformity coefficient are listed in Table 1.

### 2.2 Experimental procedure

Sand materials are completely saturated before packing to avoid entering the air and to conduct experiments under the saturated condition. In order to make homogeneous flow field, the tank is filled with water and sand of interest layer by layer in increments of 5 cm from upstream to downstream up to 100 cm to achieve uniform sand packing. For the experiments in two-layered flow field, sand comprising upstream field is packed up to 50 cm from upstream in a similar manner



of making homogeneous flow field. Then, sand is switched to make downstream flow field and is packed from 50 cm to 100 cm in the same way.

After packing sand, the water is applied to the flow tank under a specific hydraulic gradient controlled by constant head water reservoirs at upstream and downstream sides, while maintaining the saturated condition of porous media. A steady saturated flow field is established in the flow tank when fluctuation in the observed drainage rates and piezometer reading can become negligible. After reaching steady state flow condition, tracer with the volume of 20cm<sup>3</sup> is injected at the mid depth of the flow field so as not to induce complications of flow regime. During the experiment, NaCl concentration is measured with four NaCl sensors at two second intervals and the profiles of tracer migration are periodically recorded using a digital camera. Additionally, the discharge rate and piezometric water pressure are monitored over the course of the experiment to ensure that they remain constant.

### 3 Parameter estimation methods

#### 3.1 Governing equation

Contaminant transport phenomena in this experiment can be expressed by the advection-dispersion equation as follows.

$$R_d \frac{\partial c}{\partial t} = D_x \frac{\partial^2 c}{\partial x^2} + D_y \frac{\partial^2 c}{\partial y^2} + D_z \frac{\partial^2 c}{\partial z^2} - v \frac{\partial c}{\partial x} - R_d \lambda c \quad (1)$$

$$D_x = \alpha_L v, \quad D_y = \alpha_{TH} v, \quad D_z = \alpha_{TV} v \quad (2)$$

where  $c$  is solute concentration (mg/cm<sup>3</sup>),  $t$  is time (s),  $x$ ,  $y$  and  $z$  are coordinates (cm),  $R_d$  is retardation factor, and  $\lambda$  is decay constant (1/s), which is set to zero due to no biological reactions during the transport. Longitudinal dispersion coefficient  $D_x$  and transverse dispersion coefficients  $D_y$  and  $D_z$  (cm<sup>2</sup>/s) are calculated based on eqn (2). Since solute transport in this study can be seen as a two-dimensional phenomenon due to the application of tracer along with the depth, horizontal transverse dispersivity  $\alpha_{TH}$  and vertical transverse dispersivity  $\alpha_{TV}$  can be treated as the same value referred to as  $\alpha_T$ , like longitudinal dispersivity  $\alpha_L$ . During the experiments, specific velocity  $q$  (cm/s) is indirectly measured from drainage effluent and 300 cm<sup>2</sup> of cross sectional area of the flow field. Therefore, pore water velocity  $v$  (cm/s) is obtained from specific velocity divided by porosity  $n$ .

Under steady and uniform flow in  $x$  direction and a rectangular patch source having the dimensions of  $y$  and  $z$ , the solution of advection-dispersion equation



can be expressed using the analytical solution described as follows (Zheng [4]).

$$\begin{aligned}
 c = & \frac{x}{4B\sqrt{\pi D_x/R_d}} \int_0^t c_0(t-\xi) \frac{1}{\xi^{\frac{3}{2}}} \exp\left(-\lambda\xi - \frac{(x-v\xi/R_d)^2}{4D_x\xi/R_d}\right) \\
 & \left(\operatorname{erfc}\left(\frac{y-y_0}{2\sqrt{D_y\xi/R_d}}\right) - \operatorname{erfc}\left(\frac{y+y_0}{2\sqrt{D_y\xi/R_d}}\right)\right) \left((z_2-z_1) + \sum_{n=1}^{\infty} \frac{2}{n\pi/B}\right. \\
 & \left.\left(\sin\left(\frac{n\pi z_2}{B}\right) - \sin\left(\frac{n\pi z_1}{B}\right)\right) \cos\left(\frac{n\pi z}{B}\right) \exp\left(-\frac{D_z}{R_d}\left(\frac{n\pi}{B}\right)^2 \xi\right)\right) d\xi \quad (3)
 \end{aligned}$$

where  $B$  is aquifer thickness,  $y_0$  is half length of source in  $y$  direction,  $z_1$  is the bottom coordinate of  $z$  of source elevation, and  $z_2$  is the top coordinate of  $z$  of source elevation. Parameter values of  $B$ ,  $z_1$  and  $z_2$  are set to 6 cm, 0 cm and 6 cm, respectively. To reflect the experiment situation, the origin of  $x$  and  $y$  is set to the tracer injection point, while the bottom of water flow tank is  $z = 0$ . The source concentration  $c_0$  remains constant as a pulse source during a certain period, which corresponds to leak duration. Under a constraint to apply an analytical model, the source is modeled by a patch type so that leak duration is treated as a variable to be estimated, although applied tracer forms cubic source.

Table 2: Range of decision variables in GA runs.

Decision variable	Lower limit	Upper limit	Interval	Digit
$\log_{10}\alpha_L$ : (-)	-2.0	1.3	0.1	5
$\alpha_T/\alpha_L$ : (-)	0.05	0.80	0.05	4
$R_d$ : (-)	1.00	1.75	0.05	4
$t_{leak}$ : (s)	30.0	156.0	2.0	6
$y_0$ : (cm)	2.5	4.0	0.5	2

### 3.2 Inverse analysis using GA

GA is applied to estimate transport parameters. In the present study, five parameters including longitudinal dispersivity  $\alpha_L$ , the ratio of transverse to longitudinal dispersivity  $\alpha_T/\alpha_L$ , leak duration  $t_{leak}$ , source magnitude in  $y$  direction  $y_0$  and retardation factor  $R_d$  comprise an individual as shown in Table 2. Whereas the main objective of the inverse analysis is to estimate dispersivities and retardation factor, leak duration and source magnitude are included as decision variables for the purpose of calibration of a source. The selection step determines the individuals which participate in the reproduction stage and adopts tournament selection with 2 of tournament size. Reproduction step allows the exchange



of already existing genes under uniform crossover with its probability of 0.85 whereas mutation with its probability of 0.1 interchanges genes. This way of proceeding enables to efficiently arrive at optimal or near-optimal solutions. Fitness  $F$  is evaluated by the following equation, which is called objective function.

$$F = \sum_{k=1}^T \sum_{m=1}^N \left( C_{obs}^k(t_m) - C_{com}^k(t_m) \right)^2 \quad (4)$$

where  $C_{obs}^k$  is the function of space and time and means observed value of NaCl concentration at observation point  $k$ ,  $C_{com}^k$  is also the temporal and spatial function and stands for the computed value of concentration at observation point  $k$ ,  $t$  is the time when  $m$ -th datum is measured,  $T$  is the number of observation points and  $N$  is the number of observed data at each observation point. Convergence criterion is set at either  $F < 10^{-4}$  or 50 evolution of generation, resulting in 50th generation convergence for all optimal solutions.

### 3.3 Image analysis

In the process of estimation of dispersion coefficient, outlines of tracer at two different time,  $t = t_1$  and  $t = t_2$  are extracted and those centroids and coordinates composing the outline of tracer are calculated. Velocity of tracer movement in  $x$  direction  $V_{dye}$  is determined through the time  $\Delta t (= t_2 - t_1)$  and the displacement of tracer is also obtained from the spread of tracers. Consequently, the dispersion coefficient tensor related to the tracer movement during  $\Delta t$  can be computed through the following equations (Bear [5]):

$$D_{ij} = \begin{pmatrix} D_{\bar{x}\bar{x}} & D_{\bar{x}\bar{y}} \\ D_{\bar{y}\bar{x}} & D_{\bar{y}\bar{y}} \end{pmatrix} = \begin{pmatrix} \frac{1}{n} \sum_{m=1}^n \frac{\bar{x}_m^2}{2\Delta t} & \frac{1}{n} \sum_{m=1}^n \frac{\bar{x}_m \bar{y}_m}{2\Delta t} \\ \frac{1}{n} \sum_{m=1}^n \frac{\bar{y}_m \bar{x}_m}{2\Delta t} & \frac{1}{n} \sum_{m=1}^n \frac{\bar{y}_m^2}{2\Delta t} \end{pmatrix} \quad (5)$$

where  $D_{ij}$  is the dispersion coefficient tensor represented in global coordinate. The dispersion coefficient tensor in local coordinate is obtained by rotation:

$$\begin{pmatrix} D_{xx} & D_{xy} \\ D_{yx} & D_{yy} \end{pmatrix} = R D_{ij} R^T, \quad R = \begin{pmatrix} \cos \theta & \sin \theta \\ -\sin \theta & \cos \theta \end{pmatrix} \quad (6)$$

where  $T$  means the transpose matrix. The longitudinal dispersion coefficient corresponds to  $D_{xx}$  and transverse dispersion coefficient is  $D_{yy}$ . Moreover, the longitudinal and transverse dispersivities are estimated based on the relation between the tracer velocity and the dispersion coefficient as follows:

$$D_{xx} = \alpha_L |V_{dye}|, \quad D_{yy} = \alpha_T |V_{dye}| \quad (7)$$

where  $\alpha_L$  is the longitudinal dispersivity and  $\alpha_T$  is the transverse dispersivity. For the detail in this procedure with respect to image analysis technique, referred to



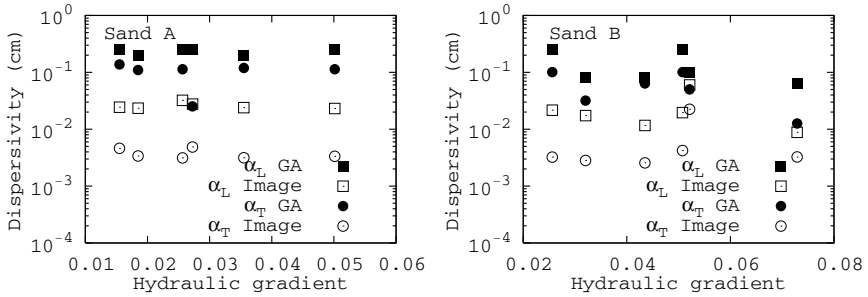


Figure 2: Dispersivity estimates in homogeneous flow fields.

Inoue *et al.* [6]. Additionally, retardation factor can be identified as the following equation

$$R_d = \frac{v}{|V_{dye}|} \tag{8}$$

where  $v$  is pore water velocity obtained from specific velocity divided by porosity.

## 4 Results and discussion

### 4.1 Parameter estimation in homogeneous flow field

The longitudinal and transverse dispersivities estimated through two methods are plotted in Figure 2 as a function of hydraulic gradient. The left and right figures indicate the result in Sand A and B, respectively. Note that “GA” and “image” stand for the values estimated by GA and image analysis, respectively.

GA estimation provides  $\alpha_L$  and  $\alpha_T$  in the range of 0.20 to 0.25 cm and 0.032 to 0.13 cm, respectively, in Sand A. The ratio of transverse dispersivity to longitudinal dispersivity ( $\alpha_T/\alpha_L$ ) ranges from 0.1 to 0.6, providing the mean value of 0.45. On the other hand,  $\alpha_L$  and  $\alpha_T$  estimates using image analysis range from  $2.3 \times 10^{-2}$  to  $3.2 \times 10^{-2}$  cm and  $3.1 \times 10^{-3}$  to  $4.8 \times 10^{-3}$  cm, respectively, resulting in about 0.15 of  $\alpha_T/\alpha_L$ . Similar tendency is shown in Sand B. GA and image analysis exhibit  $\alpha_L$  estimates in the range of 0.063 to 0.25 cm and  $8.8 \times 10^{-3}$  to  $2.2 \times 10^{-2}$  cm, respectively, while the mean  $\alpha_T/\alpha_L$  values are 0.45 and 0.20, respectively.

Huang *et al.* [1] showed 0.092 cm of longitudinal dispersivity in the long scale column experiment. Robbins [2] estimated transverse dispersivity in the range of  $3.9 \times 10^{-4}$  to  $1.3 \times 10^{-2}$  cm. The values estimated in this study are acceptable in comparison with these studies. Meanwhile, the differences between the dispersivities estimated by GA and image analysis is about one order. This is because the detectable limit of NaCl concentration is different from the extracted outline concentration of a dye tracer. Additionally, visualized dye tracer is unlikely to precisely reflect the migration in horizontal flow due to the gravity. For



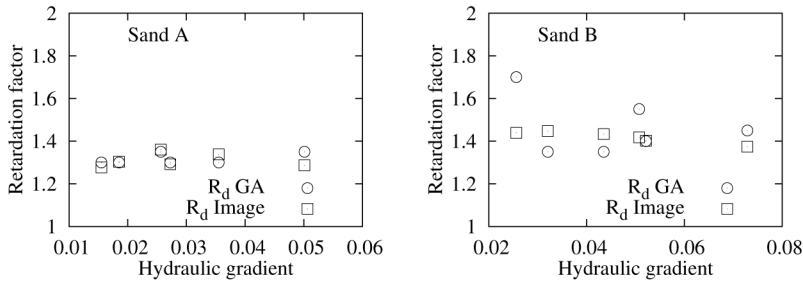


Figure 3: Retardation factor estimates in homogeneous flow fields.

these reasons, dispersivities estimated by image analysis are smaller than those estimated by GA. Moreover, two methods provide different values of  $\alpha_T/\alpha_L$ , indicating that the difficulty of accurate estimation regarding  $\alpha_T$  by GA under the measurement locations along the flow direction.

Figure 3 shows the results of retardation factor as a function of hydraulic gradient. The mean values of  $R_d$  are 1.31 in Sand A and 1.44 in Sand B. Although variation in  $R_d$  estimated by GA in Sand B is large, there is no clear differences between GA and image analysis for both in Sand A and B. This indicates that NaCl tracer as well as Brilliant Blue FCF is not a conservative tracer but is slightly absorbed and retarded by the soil. In the study of Andreini and Steenhuis [7], it is concluded that adsorption characteristics of Brilliant Blue FCF depend on soil particle size. The result obtained in this study concurs with this suggestion. Whereas, as for NaCl, similar result is reported by Rennert and Mansfeldt [8], further research is required to clarify this phenomenon.

#### 4.2 Parameter estimation in two-layered flow field

Transport parameters in two-layered flow fields are estimated using GA. As for dispersivity, it is traditionally considered possible to describe layered porous formation by means of spatial averages of the local properties over the domain. In Figure 4(a), concentration profiles corresponding the identified set of parameters in the entire domain are shown. In two-layered porous media, dispersivity in the entire domain means an equivalent parameter in conjunction with each value of the layer. Therefore, it is expected to unsatisfactorily reconstruct breakthrough curves. However, except for the lowest measurement point, the curves properly recover the concentration profiles, indicating the reliability of estimated parameters. This is because Sand A and B have a similar property regarding dispersivity as shown in Figure 2.

In order to investigate transport parameters in each layer, two breakthrough curves obtained at the upstream or downstream side are used distinctly. Recovered breakthrough curves with the set of parameters based on the breakthrough curves at the downstream layer are shown in Figure 4(b). In contrast to Figure 4(a), two



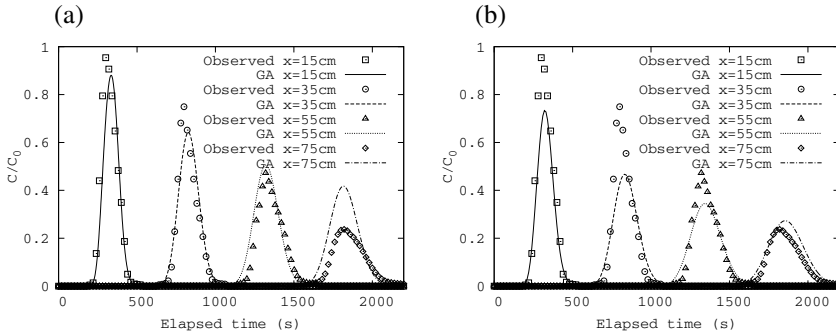


Figure 4: Recovered concentration profiles under hydraulic gradient of 0.051 in two-layered flow field. Sand B and A comprise upstream and downstream layers, respectively. (a) Result for the entire flow field. (b) Result for downstream layer.

Table 3: Result of parameter estimation in two-layered flow fields.

Layer	Upstream	Downstream	Entire field	Upstream	Downstream	Entire field
Sand	A	B		B	A	
$i$	0.016	0.048	0.029	0.044	0.016	0.028
$\alpha_L$	0.251	0.159	0.126	0.079	0.100	0.200
$\alpha_T$	0.138	0.071	0.069	0.064	0.040	0.120
$\alpha_T/\alpha_L$	0.55	0.45	0.55	0.80	0.40	0.60
$R_d$	1.30	1.35	1.30	1.35	1.35	1.35
$i$	0.019	0.053	0.035	0.052	0.019	0.036
$\alpha_L$	0.200	0.126	0.126	0.100	0.063	0.063
$\alpha_T$	0.110	0.069	0.069	0.050	0.009	0.022
$\alpha_T/\alpha_L$	0.55	0.55	0.55	0.50	0.15	0.35
$R_d$	1.30	1.35	1.30	1.40	1.50	1.50
$i$	0.027	0.076	0.051	0.073	0.029	0.051
$\alpha_L$	0.251	0.079	0.159	0.063	0.126	0.079
$\alpha_T$	0.025	0.039	0.048	0.013	0.063	0.032
$\alpha_T/\alpha_L$	0.10	0.50	0.30	0.20	0.50	0.40
$R_d$	1.30	1.35	1.35	1.40	1.45	1.40

curves at the downstream layer shows good accuracy, indicating the parameters estimated in downstream layer are different from equivalent parameters.

Table 3 shows the estimation results in two-layered flow field under the various conditions of hydraulic gradient  $i$ . Longitudinal dispersivity  $\alpha_L$  in entire field, or equivalent longitudinal dispersivity, has the tendency to be estimated between the value in upstream and downstream layer. While equivalent transverse dispersivity



$\alpha_T$  shows no specific relation with the values in upstream and downstream layer,  $\alpha_T/\alpha_L$  in entire field has the same tendency as  $\alpha_L$ , that is, the equivalent value of  $\alpha_T/\alpha_L$  exists between the value estimated in each layer. As for retardation factor, the difference of estimates appears according to the ordering of the two layers. When the upstream layer is constructed by Sand A, the retardation factor estimates range from 1.30 to 1.35. On the other hand, switching the layers leads to greater estimates of retardation factors of 1.35 to 1.50. This is attributed to the effect of the upstream layer where relatively higher concentrations are measured. From the above discussion, it is concluded that estimated dispersivities and retardation factor depend on transport pathway of contaminant in a certain degree, suggesting the importance of spatial observation location in parameter identification.

## 5 Conclusions

Laboratory tracer experiments have been conducted in 1.0 m long, horizontally placed water flow tank having cross-sectional areas of  $0.5 \times 0.06\text{m}^2$ . NaCl solution dyed with Brilliant Blue FCF has been applied in homogeneous flow fields filled with two different sand materials to simultaneously identify solute transport parameters using GA and image analysis. Moreover, experiments in two-layered media have been implemented to characterize equivalent dispersivities. The conclusions drawn from these results are the following:

1. Dispersivities estimated from image analysis is about one order smaller than those of GA estimates. In addition, the ratio of transverse dispersivity to longitudinal dispersivity is about 0.45 and 0.18 by GA and image analysis, respectively.
2. Retardation factor for both Brilliant Blue FCF and NaCl result in approximately 1.38 in this flow field.
3. Equivalent dispersivities in two-layered flow fields have a tendency to be the values between dispersivities estimated in each layer.
4. Spatially distributed observation points including transport pathway of contaminant are required to ensure the quality of the estimates.

## Acknowledgement

The study is supported, in part, by the Grant-in-Aid for Scientific Research, No. 16780169, the Ministry of Education, Culture, Sports, Science and Technology, Japan.

## References

- [1] Huang, K., Toride, N. & M. Th. van Genuchten, Experimental investigation of solute transport in large, homogeneous and heterogeneous, saturated soil columns. *Transport in Porous Media*, **18**, pp. 283–302, 1995.
- [2] Robbins, G.A., Methods for determining transverse dispersion coefficients of



- porous media in laboratory column experiments. *Water Resources Research*, **25(6)**, pp. 1249–1258, 1989.
- [3] Forrer, I., Kasteel, R., Flury, M. & Flühler, H., Longitudinal and lateral dispersion in an unsaturated field soil. *Water Resources Research*, **35(10)**, pp. 3049–3060, 1999.
- [4] Zheng, C. & Bennett, G.D., *Applied Contaminant Transport Modeling Second Edition*. John Wiley and Sons, Inc., 2002.
- [5] Bear, J., *Dynamics of Fluids in Porous Media*. Elsevier, 1972.
- [6] Inoue, K., Setsune, N., Suzuki, F. & Tanaka, T., Determining transport parameters for unsaturated porous media in flow-tank experiments using image analysis. *Proceedings of Eighth International Conference on Modelling, Monitoring and Management of Water Pollution (Water Pollution 2006) (in Press)*, WIT Press, 2006.
- [7] Andreini, M.S. & Steenhuis, T.S., Preferential paths of flow under conventional and conservation tillage. *Geoderma*, **46**, pp. 85–102, 1990.
- [8] Rennert, T. & Mansfeldt, T., Sorption and transport of iron-cyanide complexes in uncontaminated soil investigated in column experiments. *Soil Science*, **167(8)**, pp. 504–512, 2002.

